

Effect of shear rate on the performance of membrane-assisted lead acid battery

W. A. Hafiz, A. F. Ismail* and T. C. Khoo

*Membrane Research Unit,
Faculty of Chemical Engineering and Natural Resources Engineering,
University of Technology Malaysia,
81310 Skudai,
Johor Bahru, Malaysia*

Abstract

The effect of shear rate during membrane fabrication on the performance of membrane-assisted lead acid battery has been investigated. The application of lead acid battery normally faces the problem of water decomposition. This phenomenon is due to the factor of charge-discharge reaction in the battery and heat accumulation caused by hot tropical climate and heat generated from engine compartment. Gas separation membranes were prepared through dry-wet phase inversion method using various polysulfone concentrations and different shear rates. Each of these membranes was applied on the battery vent holes for the purpose of retaining electrolyte from evaporating to the atmosphere. The most suitable membrane, which retains the most electrolyte will be chosen to be applied on the soon-to-be developed membrane-assisted maintenance free battery. This maintenance free battery will not need any topping up of deionized water due to electrolyte losses. Gases emitted from both conventional and membrane-assisted lead acid batteries were analyzed with Near Infrared Fourier Transform Raman Spectrometer in order to differentiate the compositions of hydrogen and oxygen gases.

*Corresponding author: afauzi@utm.my (A.F.Ismail)

Tel: +60-7-5535592 Fax: +60-7-5581463

1. Introduction

The lead acid battery especially in tropical countries has a critical water decomposition problem that seems to be deteriorating its life cycle and performance. The combination factors of overcharging and hot weather contributed to the water losses in lead acid battery. This will be causing the decrease in electrolyte. Whenever the electrolyte level goes down, the acid concentration becomes stronger and this leads to a corrosion problem where the strong acid will attack the connector between grid and terminal and to a certain extent, the connector will break. In addition, the consumer has to top up the electrolyte level every time it goes lower than its minimum level. These are some of the problems faced in the flooded starting, lighting and ignition (SLI) batteries that need to be reviewed in its design in order to improve the performance.

Some manufacturers introduced the so-called “maintenance free” batteries that uses gelled electrolyte in their products. However, it is a disappointment that this immobilized electrolyte fails to operate in hot engine condition as reported in oriental cars, where the temperature inside the booth compartment can reach up to 60 to 80°C. Therefore, it is a thought that the application of gas separation membrane would be ideal in solving the water decomposition problem in lead acid batteries. The membrane, which acts as a selective barrier, retains electrolyte by controlling or minimizing the rate of vaporized electrolyte disposal into atmosphere.

Based on the preliminary study on the application of asymmetric polysulfone on membrane assisted lead acid battery [1], GS6 membrane has been identified as the most suitable membrane in minimizing electrolyte losses. In order to further minimize electrolyte losses in lead acid battery, the results from previous study will be improvised by manipulating fabrication condition which is the casting shear rate. Therefore, this paper is to investigate the effects of shear rate during preparation of gas separation membrane on the performance of lead acid battery.

2. Experiment

2.1. Materials

Polysulfone (Udel bisphenol A polysulfone (Udel P1700)) (purchased from Amoco Performance Products) was selected as the membrane material because of the commercial availability, ease at processing and favorable selectivity-permeability characteristics, mechanical and thermal properties, durability to high acidity conditions and its cost effectiveness. Polysulfone (PSF) is an amorphous glassy polymer, containing sulfone group, ether linkage and aromatic nuclei in polymer backbone. All the chemicals used such as *N,N*-dimethylacetamide (DMAc), dimethylformamide (DMF) ethanol and tetrahydrofuran (THF) were analytical grade and purchased from Aldrich Co. and used as received.

2.2. Membrane preparation

The membranes applied on lead acid battery were prepared by casting polymer solution consists of 13 wt/wt % of Polysulfone (PSF) and 87 wt/wt % of N-N-dimethylformamide (DMF) [1]. Casting process was performed by using a pneumatically-controlled casting machine. Casting solution was cast on a glass plate with a casting knife gap for setting of 150 μ m. In this analysis, GS6 membranes prepared at various shear rates ranging from 175 s⁻¹ to 300 s⁻¹ were tested to investigate the effect of shear rate on the performance and structure of the membranes. The membranes were cast using six different shear rates and substituted with the names as shown in Table 1.

Table 1
GS 6 membranes prepared with different casting shear rates

| Membrane Casting Shear Rate (s ⁻¹) | Substitute Name |
|--|-----------------|
| 300 | 7s |
| 262.5 | 8s |
| 233.33 | 9s |
| 210 | 10s |
| 190.91 | 11s |
| 175 | 12s |

2.3. Membrane-assisted lead acid battery charging test

The membrane will be applied into a spiral end stainless steel battery cap on battery vent hole, and then sealed with epoxy sealant to prevent any leakages. Using an alternator at the average rate of 15 Amps per hour, the battery is charged for approximately three hours. Gas permeating from the battery cap is measured as such shown in Figure 2, where it uses the principle of air bubble flow meter. During this experiment, three parameters were observed, which are the flow rate of the permeating vaporized electrolyte; the electrolyte losses and the pressure build up measure inside battery. At the end of the experiment, the membrane with the best casting shear rate will be selected and will proceed to the final stage experiment. The best casting shear will be expected to have the best performance in minimizing electrolyte losses as well as minimizing pressure build up.

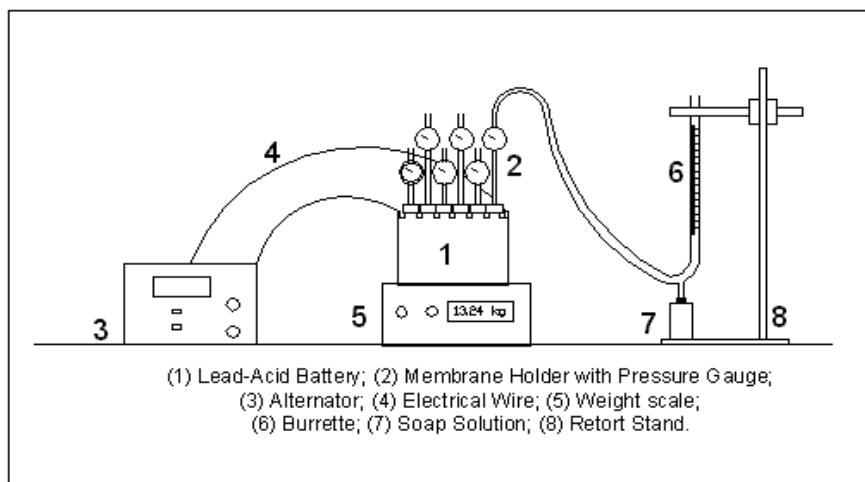


Figure 2 : Membrane-assisted lead acid battery charging test

2.4. Scanning electron microscopy (SEM) analysis

Membrane structure and morphology were examined by using scanning electron microscopy (SEM). Membrane samples chosen from different batches of membrane were fractured cryogenically in liquid nitrogen to leave an undeformed structure, and mounted on sample stubs with double-surface Scotch tape. The samples were gold coated using a sputter coater (Biorad Polaron Divison). The samples were then imaged by scanning electron microscope (Philips SEMEDAX; XL40; PW6822/10) with 20 kV potential under magnifications ranging from 250x to 300x.

2.5. Composition measurement of vaporized electrolyte with raman spectroscopy

Raman Spectroscopy was used to analyze the intensity of the vaporized electrolyte. In this case, all of the six lead acid battery caps were fitted with tubing to channel the vapor inside the battery before collected inside a glass holder. This glass holder will be placed manually in the Raman Spectrometer chamber, where the source X-ray light will be directed on the sample. Both conventional and membrane assisted lead acid batteries were charged and the vaporized electrolyte samples will collected every 20 minutes for three hours period. The Raman spectrum will feature a Raman Shift versus intensity form of data. From the spectrum, the peaks will be analyzed accordingly to the wave number and the intensity of the samples. Through this analysis, the concentration of hydrogen and oxygen molecules can be indicated through the Raman intensity peaks obtained from the spectrum [2].

3. Results and Discussion

3.1. Effect of shear rate on the performance of membrane in minimizing electrolyte losses

During membrane-assisted lead acid battery charging test, the most important parameter observed here is the electrolyte losses. This is because the main objective of this research is to minimize the electrolyte losses from the lead acid battery during charging process. One of the criteria in selecting the best shear rate for the membrane is its capability in retaining the electrolyte volume from being disposed into the atmosphere.

Figure 3 shows the profile of electrolyte losses for three selected membrane shear rates and one control test. The electrolyte loss for the control test was continuously increasing until the end of the test. At the end of the three-hour experiment, the control test battery lost about 80 grams of electrolyte, and has an average electrolyte losses rate of 26.67 grams per hour. For the membrane assisted lead acid battery, the electrolyte losses were found to be the coherent in shear rates of 7s, 11s and 12s, with the rate of losses of 20 grams per hour. Whereas for the shear rates of 8s, 9s and 10s, the average rate of electrolyte losses was minimally found to be 6.67 grams per hour.

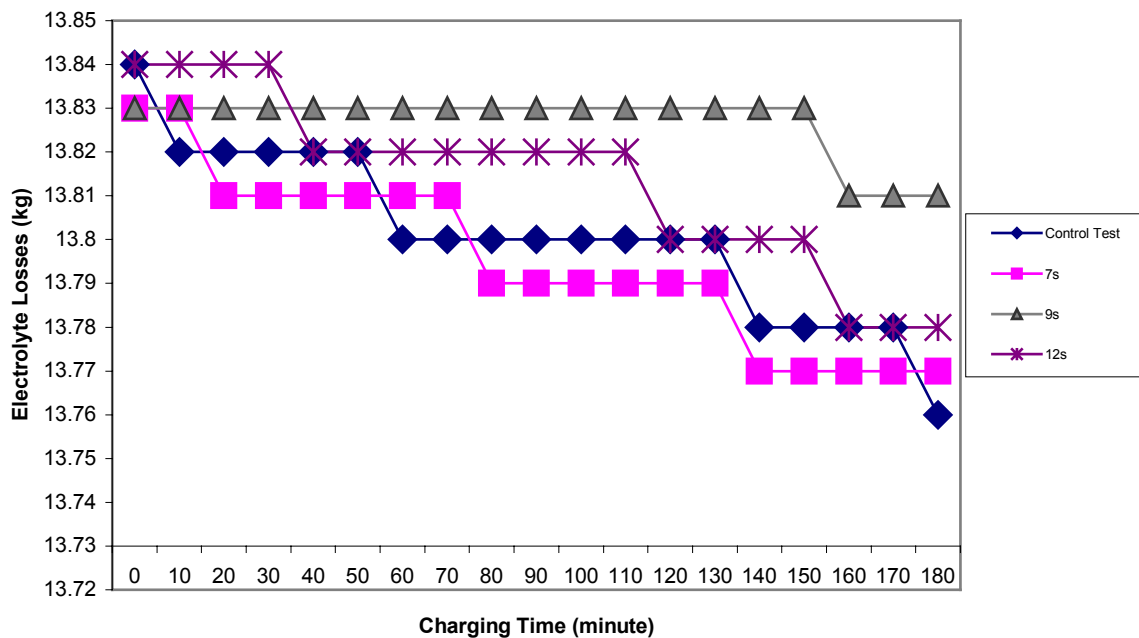


Figure 3: Effect of membrane casting shear rate on the performance of membrane in minimizing electrolyte losses

As depicted in Figure 4, the calculated percentage of electrolyte losses minimization with using GS 6 membranes cast at different shear rates compared to the conventional lead acid battery. The percentage of electrolyte losses minimization was calculated with the below equation:

$$= \frac{(\text{Electrolyte loss for control test} - \text{Electrolyte loss with membrane})}{(\text{Electrolyte loss for control test})} \times 100\% \quad (4.1)$$

Figure 4 shows that with the application of 7s, 8s and 12s membranes, the electrolyte losses can be minimized up to 25%. However, with the application of 8s, 9s and 10s membranes, the electrolyte losses can be minimized with a better percentage of 75%, which is three folds better than the latter. Even though it seems that the electrolyte losses in shear rates of 7s, 11s and 12s are still low, but they were outshone by the performance of 8s, 9s and 10s membranes. This means that the critical shear rate must lie within the range of 210s^{-1} to 262.5s^{-1} .

In order to identify the critical shear rate, a comparison analysis must be made on other parameters, which are the pressure build up inside the battery casing and the flow rate of the vaporized electrolyte profile. The critical shear rate will feature a minimal pressure build up inside the battery casing and the smoothest flow rate profile of vaporized electrolyte.

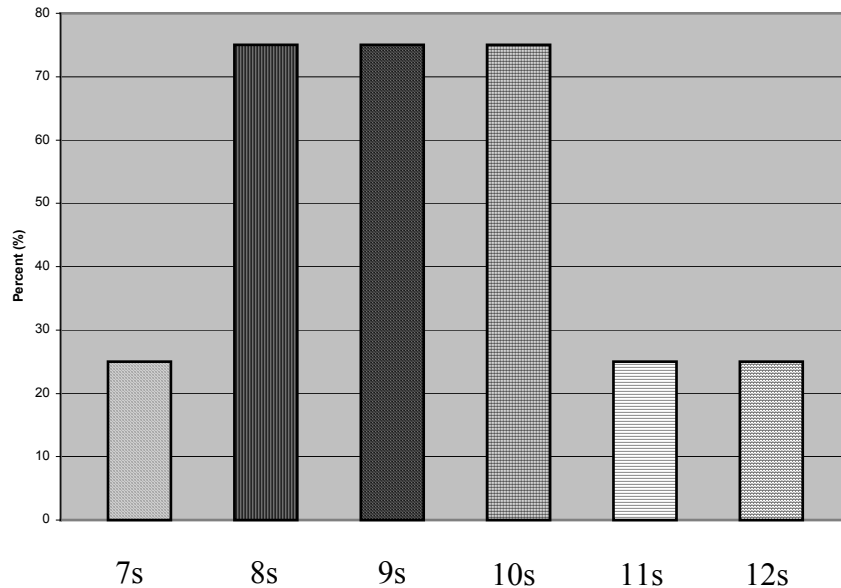


Figure 4: Minimization of electrolyte losses with comparison to the conventional lead acid battery

3.2. Effect of membrane casting shear rate on the performance of membrane in minimizing pressure build up

Figure 5 shows typical pressure profiles of pressure build up during membrane-assisted lead acid battery charging test. There is no pressure profile for the control test as there was no pressure build up since all of the vaporized electrolytes were disposed through the vent hole.

Membranes cast at six different shear rates show different values of maximum pressure build up with similar trend of profile. Each of the membranes had a sudden increase of pressure build up during the first twenty minutes of charging. The next phenomenon seen after the sudden increase is the pressure build up starts to show tendency in becoming constant as the flow rate of vaporized electrolyte becomes faster.

During the first twenty minutes of charging, the vaporized electrolyte could not be permeated smoothly since the pressure build up is still low. Since membrane flux is pressure driven, the vaporized electrolyte could not permeate through the selective skin and therefore trapped inside the battery casing. The pressure build up has increased until it reaches the point where the pressure becomes constant and the vaporized electrolyte permeation rate becomes constant too. This is the point when the condition reaches its “working pressure”, where the pressure build up is stabilized with the smooth and constant permeation of vaporized electrolyte.

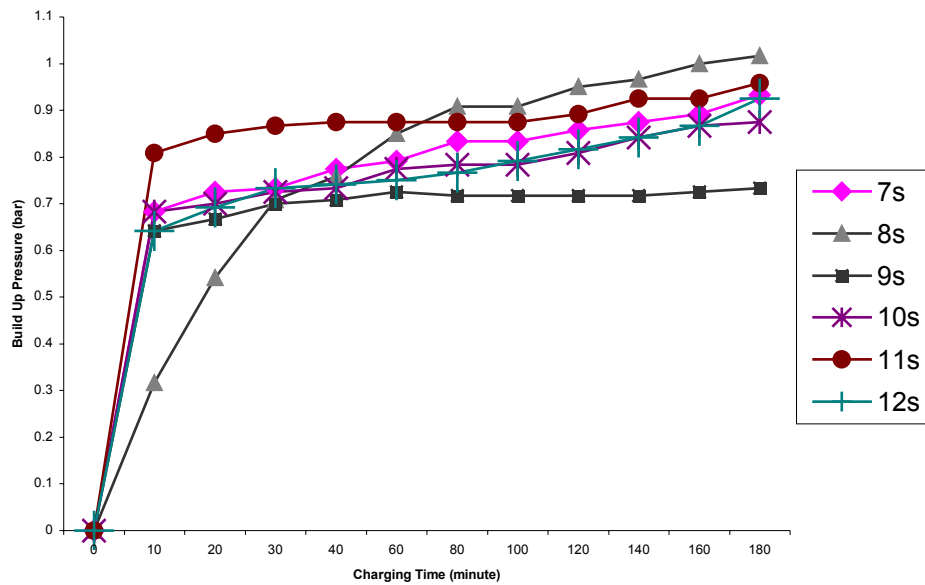


Figure 5: Effect of casting shear rate on the pressure build up inside battery casing

In selecting the critical shear rate within the six different shear rates applied, the pressure profile must feature a minimum value of “working pressure” as well as minimizing electrolyte losses during the charging process. In this case, the 9s membrane (cast at 233 s^{-1}) had the lowest pressure build up profile with the final build up pressure of only about 0.73 bar after three hours of charging. Compared to the other shear rates, 7s

membrane recorded about 0.93 bar; 8s membrane about 1.02 bar; 10s membrane about 0.88 bar; 11s membrane about 0.96 bar and 12s membrane about 0.93 bar, 9s membrane relatively has the lowest final pressure.

As shown in Figure 6, the flow rate of gas permeation from the battery during charging in the control test is continuously increasing. This shows that, electrolyte is continuously decomposed without application of membrane. Most of the membranes have shown a slow increase of vaporized electrolyte flow rate except for 9s membrane. The rate of increment for vaporized electrolyte flow rate in 7s, 8s, 10s 11s and 12s membranes are not that distinct from what had been shown in the 9s membrane flow rate profile. The flow rate of gas permeation from the battery during charging with the application of 9s membrane is quite slow at the early stages of charging and the rate is increasing as time elapse. During the first sixty minutes of charging, 9s membrane have shown slower flow rate of vaporized electrolyte due to its electrolyte retaining characteristic. However after the first sixty minutes, 9s membranes profile almost emulates the flow rate of the control test, and this proves that the vaporized electrolyte is being well circulated inside the battery without tolerating the minimization of electrolyte losses during charging. This indicates that as charging goes along the way, the permeation of gas will continuously increase and pressure build up inside the battery casing could be minimized.

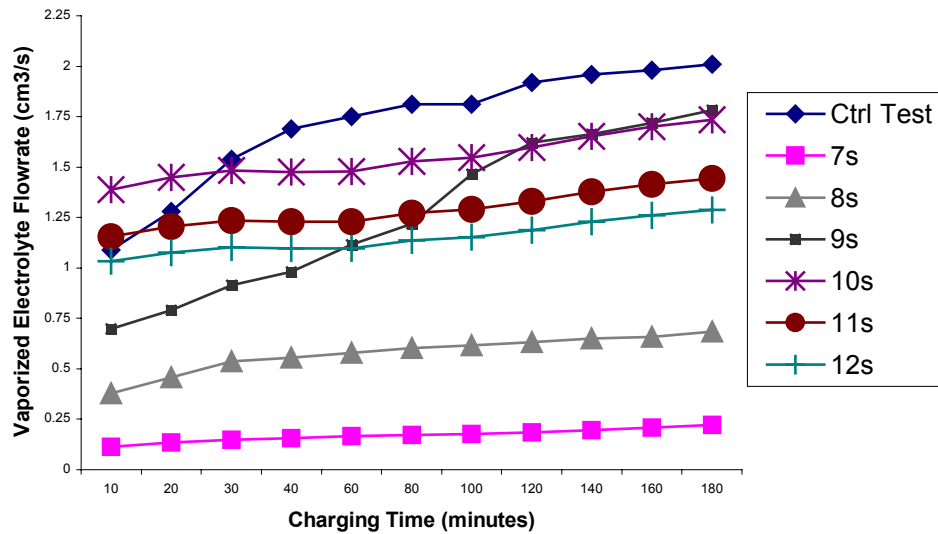


Figure 6: Effect of casting shear rates on the flow rate profile of vaporized electrolyte

Effect of shear experienced in casting process on membrane properties were intimately correlated to the structural knowledge at molecular level. As shown in Figure 4 and 5, the critical shear is selected for the performance analysis of each of the shear rates in minimizing electrolyte losses as well as in minimizing pressure build up during charging process. Based on the results obtained, the critical shear rate was determined to

be about 233.33 s^{-1} for 9s membrane, due to its minimal electrolyte losses and lowest pressure build up showed among the other shear rates.

In the region prior to the critical shear rate (233.33 s^{-1}), formation of dense skin occur due to demixing and precipitation mechanism, which was considered to be independent of shear rate. Increasing shear rate enhance molecular orientation in skin layer and in turn, improving selectivity in asymmetric membrane [3, 4]. This has been demonstrated where electrolyte losses were seems to be further minimized. The permeation rate of asymmetric membrane was also found to increase when the shear rate is approaching to the critical shear. This was consistent with the reduction in skin thickness, where increasing shear rate seems to decrease skin layer thickness and the pressure build up seems to be lowered [5].

Since the solution used in this study is shear thinning, when shear rate reached beyond the critical point (233.33 s^{-1}), a severe decrease in solution viscosity occurred presumably due to losses in chain entanglement in solution. In this case, membrane might undergo an instant demixing and precipitation to result in a highly oriented skin layer. [6,7]. Furthermore, casting over the critical shear rate (233.33 s^{-1}) which is considered high shear rate, could pull molecular chains or phase separated domains apart and began to create slight defects or imperfections in skin layer [6]. As shown in the Figure 5, casting polysulfone membrane at higher shear rates (262.15 s^{-1} to 300 s^{-1}) causes a decrease in selectivity where electrolyte losses seems to be higher than those featured near the critical shear rate region.

Figure 7 and Figure 8 showed the overall intensities for hydrogen and oxygen gases during the three hour charging process. As depicted in the Raman spectrums, the Raman shift (wave number) for the detected hydrogen and oxygen intensity peaks would not only found at 4155 cm^{-1} and 1555 cm^{-1} respectively, but it could also found at regions near to these two plots. This phenomenon occurred due to the fact that gas samples were having high kinetic energy. Therefore, the mobility of the molecules forces of the scattering process occurred at different Raman shifts. However, it was still in the near regions of the normalized differential Raman scattering cross section.

As depicted in Figure 7, the intensities for hydrogen in conventional battery gas samples were seems to be marginally high when compared to the intensities found in the membrane-assisted lead acid battery. It can be determined that, the intensities for conventional battery gas samples were mostly 50 to 60% higher than those found in the membrane-assisted battery gas samples. These intensities indicated the concentration of hydrogen gas contained in the gas samples and simultaneously showed that most of hydrogen gas evolved during charging process were still retained in the membrane-assisted battery.

Figure 8 shows a similar phenomenon of hydrogen intensities, where the oxygen intensities for conventional battery gas samples were higher compared to the intensities found in the membrane-assisted battery. As calculated, the intensities for oxygen gas samples in conventional battery were about 10 to 30% higher compared to the

membrane-assisted battery gas samples. The vaporized electrolyte in membrane-assisted lead acid battery had lower oxygen concentration due to the fact that most of the oxygen gas evolved during charging process were being retained in the battery casing.

These scenarios indicated that the concentration of hydrogen and oxygen in conventional battery are higher than that of membrane-assisted battery. The explanation to this phenomenon is that most of the hydrogen and oxygen gases evolved during charging process are being retained inside the membrane-assisted battery instead of evaporating freely as in the conventional battery. The application of membrane on lead acid battery during charging seems to lowering the rate of vaporized electrolyte disposal into the atmosphere and to a certain extent, has successfully functioning as an electrolyte retaining device for lead acid battery. Therefore, this demonstrated that the membrane has given a significant effect in minimizing electrolyte losses in lead acid batteries during charging process.

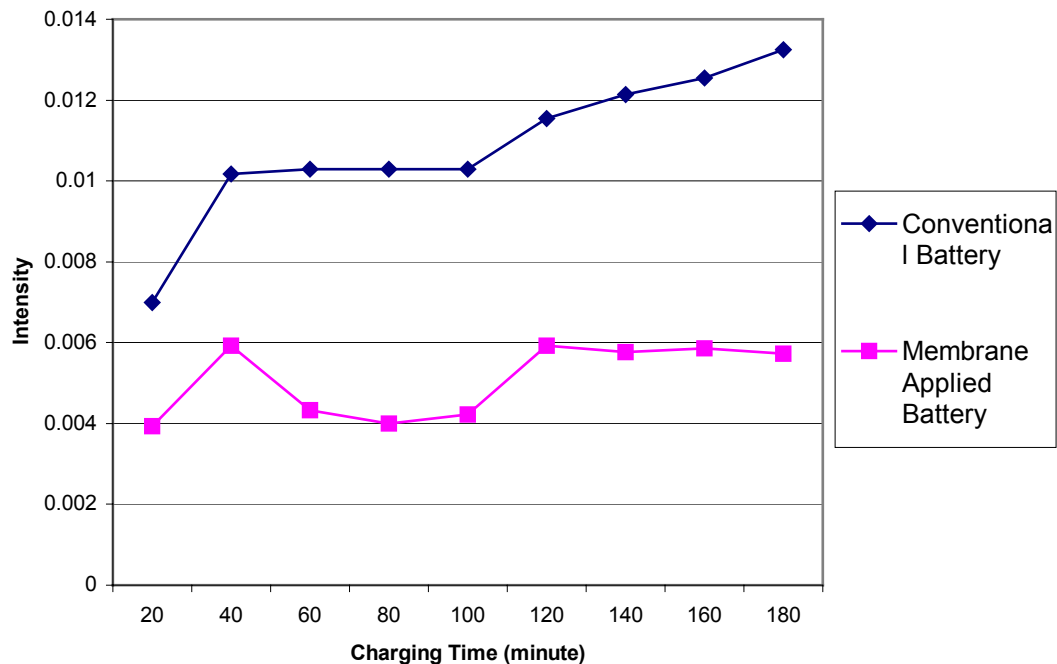


Figure 7: Overall hydrogen intensities for vaporized electrolyte gas samples for conventional and membrane applied lead acid batteries.

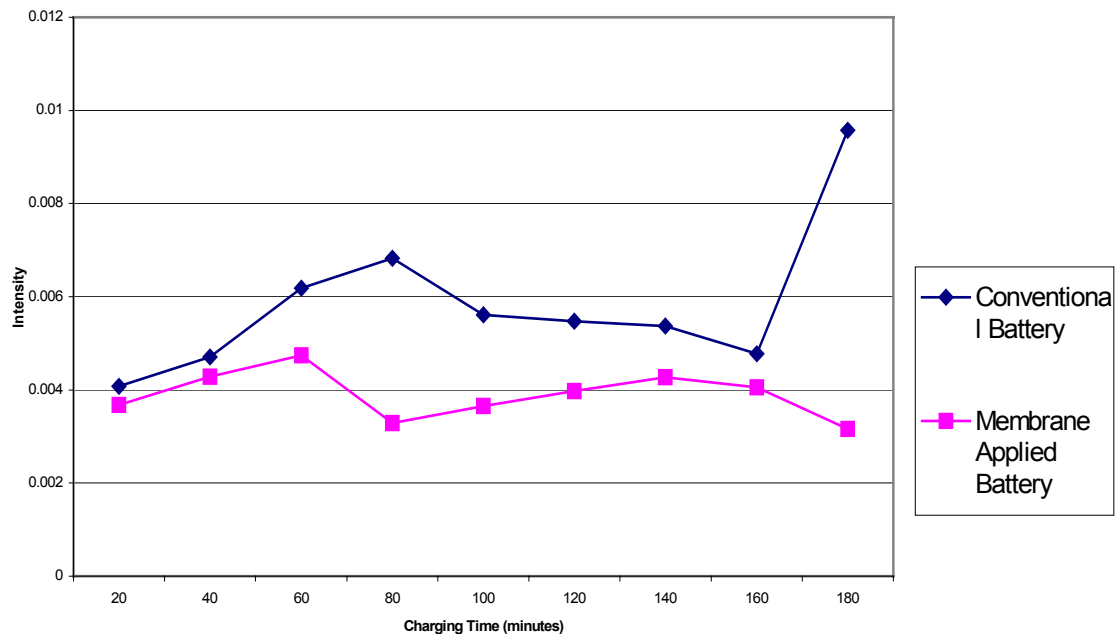


Figure 8: Overall oxygen intensities for vaporized electrolyte gas samples for conventional and membrane applied lead acid batteries

The electron micrographs of the membranes cross sections are shown in Figure 9. As expected, the developed asymmetric polysulfone membrane was composed of an ultrathin, dense skin layer with a sponge-like porous substructure, as observed in the Figure 9(a-c). However, the skin thickness of membrane was found to be decreasing with the increase of shear rate during casting process. In addition to this, as seen in Figure 9(c), a relatively thicker transition layer was found existing in the polysulfone membrane with the casting shear rate of 300 s^{-1} . There was not much of a difference in the outlook of substructures for the membranes cast at different shear rates. However, casting over the critical shear rate (233.33 s^{-1}) which is considered high shear rate, could pull molecular chains or phase separated domains apart and began to create slight defects or imperfections in skin layer and the substructure itself. As shown in Figure 9 (c), the void in the substructure of the membrane cast over the critical shear rate were uniformly arranged compared to that shown in Figure 9(b) where most of the voids were thoroughly arranged.

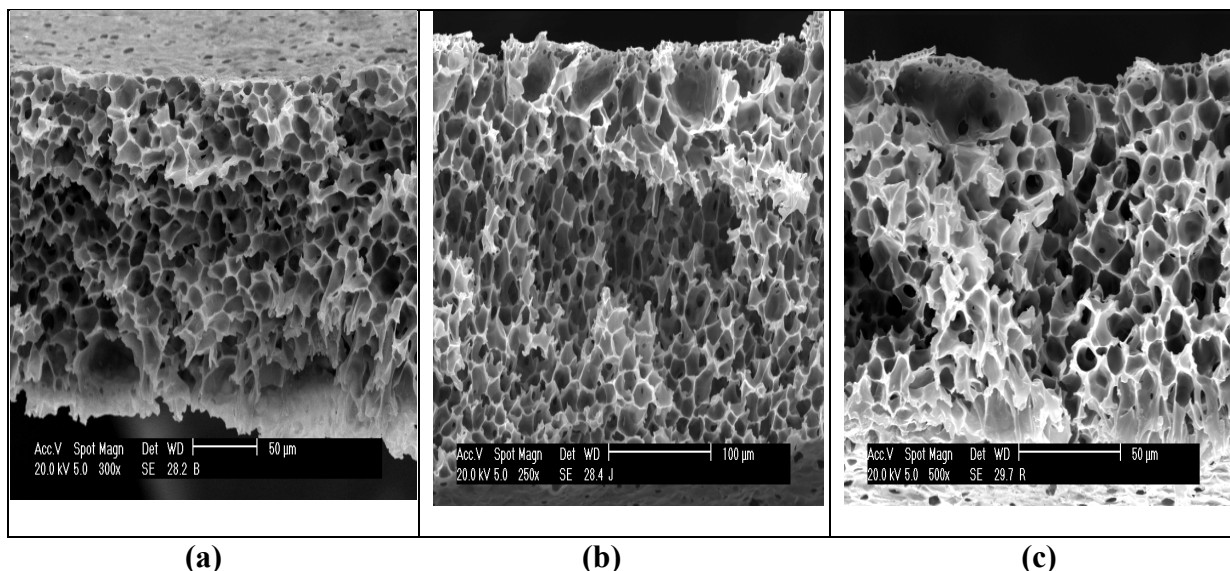


Figure 9: Scanning electron micrographs of membrane cross section with different shear rates (a: 210 s^{-1} ; b: 233.33 s^{-1} ; c: 300 s^{-1})

4. Conclusion

This study showed that shear rate during membrane fabrication played an important role in determining the performance of a membrane assisted lead acid battery. During the lead acid battery charging test, all of the membranes have successfully functioning as a good water retaining device, where electrolyte losses have been minimized and the pressure build seems to be reduced at critical shear rate. Permeation rate of vaporized electrolyte were increased with increasing shear rate and pressure build up were minimized due to reduction of skin layer thickness. Membrane cast at 233.33 s^{-1} was selected as the critical shear rate because it showed minimized electrolyte losses as well as featuring the lowest pressure build up during lead acid battery charging process.

References

- [1] Ismail, A. F., Hafiz, W. A. (2002), "Effect of Polysulfone Concentration on the Performance of Membrane-assisted Lead Acid Battery.", *Songklanakarin Journal of Science and Technology*, 24, 815-821
- [2]. Henn, F. E., Rouvet, C., de Guibert, A., Martue, P., (1996), "Hydrogen and Oxygen Evolution in Sealed Laed/acid 2V Cells. In situ Gas Measurement By Raman Spectroscopy.", *Journal of Power Sources*, 63, 235-246
- [3]. Ismail, A. F., Shilton, S. J., Dunkin, I. R., Gallivan, S. L. (1997), "Direct Measurement of Rheologically Induced Molecular Orientation in Gas Separation Hollow Fiber Membranes and Effects on Selectivity.", *Journal of Membrane Science*, 126, 133-137

[4]. Shilton, S. J., Ismail, A. F., Dunkin, I. R., Gallivan, S. L., Gough, P. J. (1997), "Molecular Orientation and the Performance of Synthetic Polymeric Membranes for Gas Separation.", *Polymer*, 38, 2215-2220

[5]. Shilton, S. J., Bell, G., Ferguson, J. (1994), "The Rheology of Fiber Spinning and the Properties of Hollow Fiber Membranes for Gas Separation." *Polymer*, 37, 5327-5335

[6]. Sharpe, I. D., Ismail, A. F., Shilton, S. J. (1999), "A Study of Extrusion Shear and Forced Convection Residence Time in Spinning of Polysulfone Hollow Fiber Membranes for Gas Separation." *Separation and Purification Technology*, 17, 101-109

[7]. Chung, T. S., Lin, W. H., Vora, R. H. (2000), "The Effect of Shear Rates on Gas Separation Performance of 6FDA-Durene Polyimide Hollow Fibers." *Journal of Membrane Science*, 167, 55-66